

RSC Advances



This is an *Accepted Manuscript*, which has been through the Royal Society of Chemistry peer review process and has been accepted for publication.

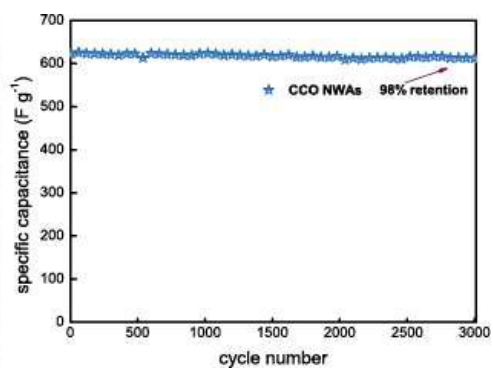
Accepted Manuscripts are published online shortly after acceptance, before technical editing, formatting and proof reading. Using this free service, authors can make their results available to the community, in citable form, before we publish the edited article. This *Accepted Manuscript* will be replaced by the edited, formatted and paginated article as soon as this is available.

You can find more information about *Accepted Manuscripts* in the [Information for Authors](#).

Please note that technical editing may introduce minor changes to the text and/or graphics, which may alter content. The journal's standard [Terms & Conditions](#) and the [Ethical guidelines](#) still apply. In no event shall the Royal Society of Chemistry be held responsible for any errors or omissions in this *Accepted Manuscript* or any consequences arising from the use of any information it contains.

Graphical abstract

Grass-like CuCo_2O_4 nanowire arrays (CCO NWAs) supported on nickel foam, just like plants growing on the soil, were prepared through a facile hydrothermal process. The stability of the morphology makes the CCO NWAs a promising electrochemical performance.





Grass-like CuCo_2O_4 Nanowire Arrays Supported on Nickel foam with High Capacitances and Desirable Cycling Performance

Received 00th January 20xx,
Accepted 00th January 20xx

DOI: 10.1039/x0xx00000x

Huaiyuan Chen, Xiaohua Chen*, Ying Zeng, Shanliang Chen and Jiande Wang

www.rsc.org/

Grass-like CuCo_2O_4 nanowire arrays supported on nickel foam have been successfully synthesized via a hydrothermal method. Electrochemical investigations demonstrate an excellent material for supercapacitor with remarkable performance including high area capacitance of 611 F g^{-1} at a current density of 1.7 A g^{-1} , desirable cycling stability of 94.8% capacitance retention after 8000 cycles.

Supercapacitors is a new kind of energy storage device.¹⁻⁴ As yet, a variety of materials such as carbonaceous materials, metal oxides/hydroxides and conducting polymers are used as supercapacitor electrode materials.⁵⁻⁶ Among the many kinds of electrode materials that candidate for supercapacitors, ternary cobalt-based spinel oxides have been actively pursued due to their better electroactivity and superior supercapacitive properties than single cobalt oxides.⁷⁻⁹ During supercapacitors research, the theoretical capacitance of a certain active material was calculated by the equation: $C = n F / (\Delta V M)$, where n is the moles of charge transferred per mole of the test substance, F is Faraday's constant ($96485.3383 \text{ C mol}^{-1}$), M is the molar mass of the test substance, and ΔV is the potential sweep range. By Calculating through the equation, we found that the CuCo_2O_4 owns a theoretical capacitance of 984 F g^{-1} . Moreover, other features, including low cost, abundant resources, and environmental friendliness, make CuCo_2O_4 a promising pseudocapacitive electrode. Up to now, there are few reports about CuCo_2O_4 applications as supercapacitor. In 2014, Afshin Pendashteh, Mir F. Mousavi et al reported CuCo_2O_4 nanoparticles with a specific capacitance of 338 F g^{-1} at current densities of 1 A g^{-1} .¹⁰ However, owing to the high surface energy, nanoparticles always tend to self-aggregation, which reduces the effective area of the electrode/electrolyte interface. Also, these materials suffer from severe volume variation during charge discharge cycling, which results in serious pulverisation of the electrodes and thus rapid capacity degradation. Therefore, it is

crucial to retain the large contact area to fully fulfill the advantages of active materials and to inhibit volume change of these materials during cycling. Recently, constructing three-dimensional (3D) architectures based on two-dimensional (2D) substrates has been proved to be an effective approach to solve these problem.¹¹⁻¹⁴

In this communication, we developed a cost-effective and simple strategy for direct growth of hierarchical CuCo_2O_4 (CCO) nanowire array (NWAs) on a nickel foam substrate as a binder-free electrode for high-performance supercapacitors. In such structures, the CCO NWAs grown on Ni foam could effectively avoid the aggregation of active materials and provide more active sites for electrochemical reaction. The existence of the spacing between each nanowire of about 50 nm and the ultra-thin nanowires can provide a short ion diffusion path and facilitate fast transport of ions during charge-discharge process. In addition, Ni foam act as an excellent backbone for loading CCO nanowire array and a highly conductive matrix for them. Since Ni foam can provide pathways for electronic transport, it can serve as the current collector without conductive additives. This binder-free electrode by directly growing active materials on 3D Ni foam simplifies the procedure for electrochemical measurement, which is helpful in practical applications. The combination of these constituents is expected to display highly effective electrochemical properties. As a result, CCO NWAs exhibit high specific capacitance (611 F g^{-1}), and excellent cycle stability

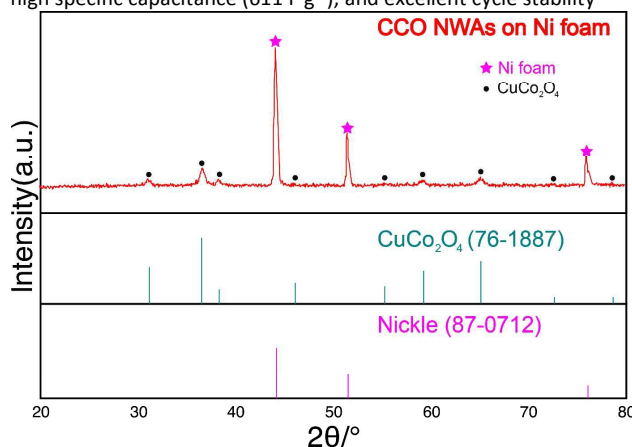


Figure 1 XRD pattern of CCO NWAs on Ni foam.

College of Materials Science and Engineering, Hunan University, Hunan Province
Key Laboratory for Spray Deposition Technology and Application, Changsha
410082, China

E-mail: xiaohuachen@hnu.edu.cn

Electronic Supplementary Information (ESI) available: [details of any supplementary information available should be included here]. See
DOI: 10.1039/x0xx00000x

(94.8% capacitance retention after 8000 charge-discharge cycles) in a 2M KOH solution.

In order to confirm the phase structure of the products, the XRD measurements were carried out. As shown in Figure 1 all of the diffraction peaks of the CCO NWAs can be indexed to CuCo_2O_4 according to Joint Committee on Powder Diffraction Standards (JCPDS, card No. 76-1887). Besides, the three peaks around 44.3° , 51.6° and 76.1° were also observed, coming from the Ni foam (JCPDS, card No. 87-0712). No other impurities peaks were observed, implying the products with high purity.

The morphology of bare nickel foam and CCO NWAs covered Ni foam examined by SEM was shown in Figure 2 a-d. The submillimeter pores and nickel foam skeletons can be clearly seen in Figure 2a. Figure 2b-d displays the SEM images of the obtained CCO NWAs on Ni foam. From the distant view, it can be seen the Ni foam surfaces are uniformly covered with product as shown in Figure 2b. The close views of the CCO nanowires in Figure 2c-d indicate that the nanowires lie perpendicular to the Ni foam support, forming an ordered nanoarray structure. The higher magnification SEM image (Figure 2d) discloses the space of approximately 50 nm between nanowires, thus, most of the nanowire surface is highly accessible by the electrolyte when used as an electrode for supercapacitors.¹⁶

Figure S1a and b are the side views of the substance under SEM. From these figures we can clearly see the previously prepared CCO NWAs with a length of approximately 3 μm and thickness of approximately 100 nm. More distinctly, from Figure S1c, we learned that the CCO NWAs supported on nickel foam are just like grass growing on the ground. Obviously, such a large area of one-dimensional nanowires can greatly enhance the specific surface area of the CCO NWAs, leading directly to the increased contact

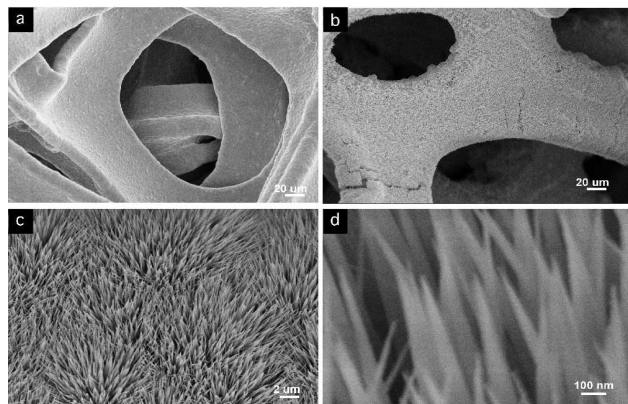


Figure 2 SEM characterizations of the morphologies of the CCO NWAs on Ni foam. (a) bare Ni foam; (b) Ni foam after hydrothermal reaction; (c) and (d) higher resolution images of CCO NWAs.

area between the electrolyte and the active material. By direct growth on foam nickel, the nanowires are well-separated, making them fully available to the OH^- in the solution, resulting in a high utilization of materials. Third, the nanoscale space between nanowires (about 50 nm) possesses a favorable morphological stability, helping to alleviate structure damage caused by volume expansion during cycling. What's more, inherent contact between nanowires and nickel foam avoids the need for binders and

conducting additives that add extra contact resistance or weight.¹⁷ Thus an effective and stable pathway for charge transfer

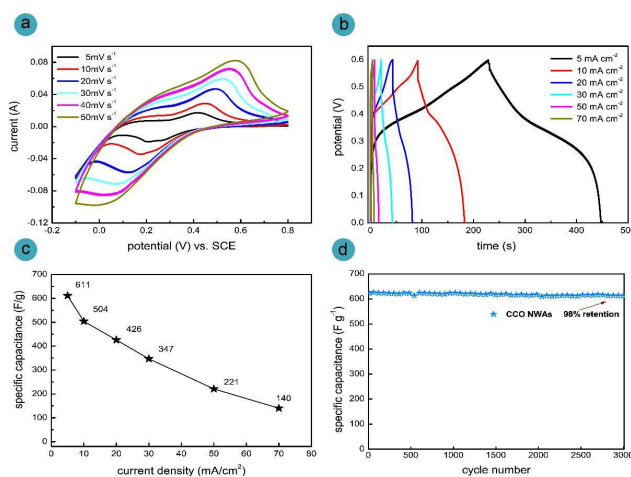


Figure 3 Electrochemical characterization of CCO NWAs on Ni foam: (a) CV curves at different scan rates, (b) galvanostatic charge/discharge curves at different current densities, (c) The Current density dependence of the specific capacitance calculated from the discharge curves and (d) cycling performance at current density of 5 mA cm^{-2} .

could be formed. From the above, the CCO NWAs supported on nickel foam are expectable to provide high performances.

To test the electrochemical capacitive performance of CCO NWAs, cyclic voltammogram (CV) was firstly recorded in a three-electrode system using SCE as the reference and platinum foil as the counter-electrode in 2M KOH aqueous at room temperature. Figure 3a reveals the typical CV curves of as-prepared CCO NWAs with the potential window -0.2 to 0.8 V (vs. SCE) at various scan rates ranging from 5, 10, 20, 30, 40 to 50 mV s^{-1} , respectively. All the CV curves consist of a pair of strong redox peaks, indicating that the capacitance of the materials is mainly associated with Faradaic pseudocapacitor, which are quite different from curves of electric double layer capacitors. Moreover, the shape of the CV curves was not affected by the increase of the scan rate, indicating that this unique structure favors fast redox reactions. Nearly symmetrical shapes observed under different scan rates imply an ideal pseudocapacitive behavior for CCO NWAs.¹⁸ The specific capacitance (C) was calculated according to the following equation:²⁵

$$C = \frac{\int i x d\Delta u}{v \times \Delta u \times m}$$

where Δu is the potential (V), v is the potential scan rate (mV s^{-1}), i is the discharging current (A), and m represents the active mass (g). Based on the equation the surface capacitance values can be calculated to be 361.41, 331.27, 294.38, 253.67, 234.00 and 211.61 F g^{-1} at scan rates of 5, 10, 20, 30, 40 and 50 mV/s , respectively. Taking the geometrical area of the electrode of CCO NWAs into account ($1 \times 1 \text{ cm}^2$), the specific capacitance values are $1.08, 0.99, 0.88, 0.76, 0.70$ and 0.63 F cm^{-2} , respectively (Figure S5). For comparison, the bare Ni foam without hydrothermal reaction after annealing procedure in pure N_2 gas was also investigated in the same system. It can be found that the capacitance contribution from Ni foam substrate is negligible, as shown in Figure S2.

Figure 3b displays the galvanostatic charge-discharge behavior of the CCO NWAs as electrode at different current densities in the potential range between 0 and 0.6 V. The symmetry of the charge and discharge curves exhibit excellent reversible forward and backward reaction process. The specific capacitances of CCO NWAs at different charge and discharge current density were calculated as shown in Figure 3c according to the equation: $C = I t / (m \Delta V)$. I is the constant discharge current, t is the discharge time, ΔV is the voltage drop upon discharging and m is the mass of active materials. The mass of CCO NWAs was 3 mg/cm^2 and it was taken into account to calculate the specific capacitance and current density. The CCO NWAs electrode exhibits a superior pseudocapacitance of 611, 504, 426, 347, 211 and 140 F g^{-1} at current densities of 1.7, 3.4, 6.7, 10, 16.7 and 23.3 A g^{-1} , respectively. It can be seen that increasing the specific current

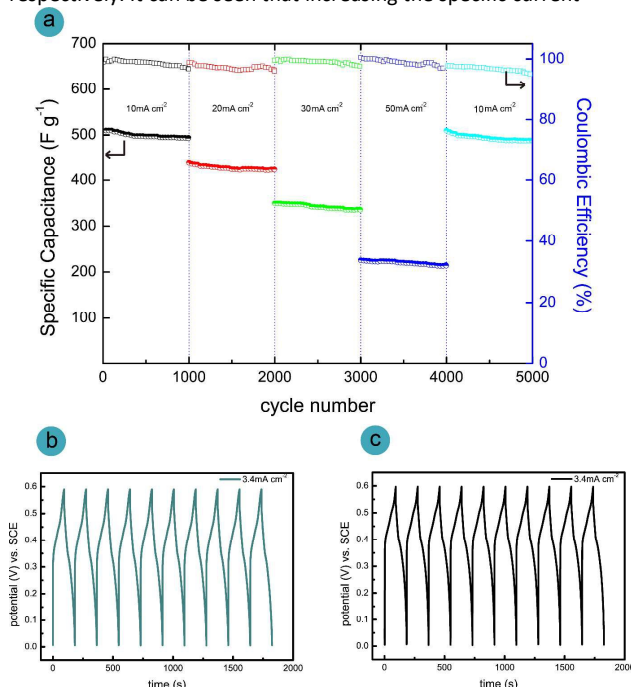


Figure 4 (a) Rate performance of the CCO NWAs on Ni foam electrodes at progressively increased current densities; (b) and (c) corresponding charge/discharge curves of the first 10 and last 10 cycles of the CCO NWAs on Ni foam electrode for the 5000 cycles.

results in a decrease in a specific capacitance, in agreement to the trend of capacitance variation calculated from CV curves.

The CCO NWAs exhibit a specific capacitance as high as 611 F g^{-1} at a charge and discharge current density of 1.7 A g^{-1} , higher than 338 F g^{-1} at current densities of 1 A g^{-1} reported by Afshin Pendashteh, Mir F. Mousavi et al. Even at a high charge and discharge density of 23.3 A g^{-1} , a specific capacitance of 140 F g^{-1} can also be achieved, implying that the CCO NWAs has a relatively good rate capability at a large specific current (Figure 3c). The cycling performance is a desirable parameter for supercapacitor performance to replace the lithium-ion battery.¹⁹ Large capacitance retention over prolonged charge discharge cycle is essential for outstanding electroactive material. Figure 3d represents few capacitance losses after 3000 cycles at a current density of 5 mA cm^{-2} . After 3000 cycles at 5 mA cm^{-2} , the specific capacitance remains 98% of the initial value,

shown in Figure 3d. For supercapacitor, long cycle life and high rate capability are important parameters for its practical application.²⁰ Following the above 3000 cycles, the electrode is subjected to continuous discharge-charge process for 5000 cycles at different current densities. As shown in Figure 4a, during the 4000 cycles with the current densities increasing from 10 to 20, 30, 50 mA cm^{-2} , the electrode exhibits a perfect capacitance stability and the capacitance retention are more than 94.8%. When the current density comes back to 10 mA cm^{-2} , a capacitance of 95.8% of the initial 1000 cycles under 10 mA cm^{-2} (shown in figure 4b, blue curve) is observed, and have a capacitance retention of 96% during another 1000 cycles. The good stability of the as-prepared CCO NWAs with high specific capacitance makes them a promising candidate for potential application in supercapacitors. Besides, it is also noticed that the specific capacitance is about 60% of the theoretical capacitance (984 F g^{-1}). These results indicate that the 1D nanowires and their separate morphology from each other on growth substrate of 3D configuration can effectively prevent the volume expansion, contraction and aggregation of the electroactive materials during charge-discharge process.

We also use the electrochemical impedance spectroscopic (EIS) measurements to further investigate the electrochemical behavior of CCO NWAs at open circuit potential with an AC perturbation of 5 mV in the frequency ranging from 0.01 Hz to 100 KHz before and after cycling. Generally, Nyquist plots contain a semicircle and a straight line.²¹ In low frequency area, the slope of the curve shows the Warburg impedance (W) which represents the electrolyte diffusion in the porous electrode and proton diffusion in host materials.²² Figure 5a compares the Nyquist plots of CCO NWAs electrodes before and after 3000 cycles at a current density of 5 mA cm^{-2} with a well-fitted equivalent circuit showing the components of the whole impedance.²³ Apparently, the slope of the curve after cycling barely changes compared with that before cycling. In the high frequency area, the intersection of the curve at real part Z' indicates the bulk resistance of the electrochemical system and the semicircle displays the charge-transfer process at the working electrode-electrolyte interface.²⁴ From this plot, the impedance of the as-prepared sample changes little after 3000 cycles, which further certifies that the CCO NWAs has a lower diffusion resistance and stable electrochemical property. Figure 5b is the schematic illustration of electron path about the CCO NWAs on Ni foam, which provides considerably shorter paths for electron transport and a solid structure to improve their capacitive performance. In practice, the CCO NWAs produce more ion migration channels to promote the electrolyte ion transport in three-dimensional space, not just at the edge of the CuCo_2O_4 NWAs. For comparison, the CVs, CPs and EIS of pristine Ni foam are shown in the electronic supplementary information, Figure S2 and Figure S4. It can be found that the capacitance contribution from Ni foam substrate is negligible.

COMMUNICATION

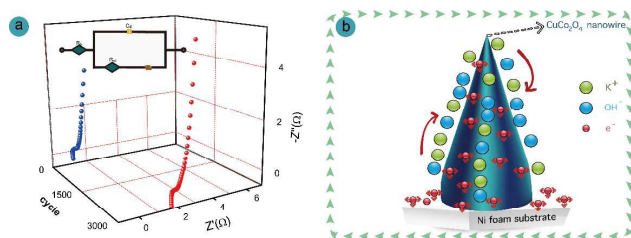


Figure 5 (a) Electrochemical impedance spectra (EIS) of the CCO NWAs on Ni foam electrodes. The blue curve refers to the EIS before cycling, and the red curve is the EIS after 3000 cycles. The inset is the equivalent circuit; (b) schematic representation of rechargeable supercapacitor based on CCO NWAs on Ni foam.

Conclusions

In summary, we have illustrated the logical design and fabrication of CuCo_2O_4 (CCO) nanowire arrays on Ni foam substrate using a facile hydrothermal method without any surfactant and template. The CCO NWAs supercapacitor electrode exhibits extraordinary electrochemical property in terms of cyclic stability and rate performance, and particularly, the specific capacity is 60% of the theoretical capacitance of 984 F g^{-1} . The prodigious performance is attributed to the superiority of the high specific surface ratio of 1-D nanowire and 3-D soil for growth (Ni foam), which makes ion transport easily within and between the electroactive materials.²⁵⁻²⁶ Otherwise, the freestanding and binder-free nature of the materials make it have broader applies.²⁷ To sum up, this material made from abundant, low-cost precursors along with the facile synthesis technique making it an ideal candidate for next-generation supercapacitor electrodes. The experiments results are inspiring considering that the electrodes have more space for the development of applications.

Notes and references

- 1 P. Simon and Y. Gogotsi, *Nat. Mater.*, 2008, 7, 845.
- 2 I. E. Rauda, V. Augustyn, B. Dunn, S. H. Tolbert, *ACCOUNTS CHEM RES*, 2013, 46, 1113.
- 3 V. Augustyn, P. Simon, B. Dunn, *ENERG ENVIRON SCI*, 2014, 7, 1597.
- 4 B. E. Conway, V. Birss, J. Wojtowicz, *J POWER SOURCES*, 1997, 66, 1.
- 5 L. Hao, X. Li, L. Zhi, *ADV MATER*, 2013, 25, 3899.
- 6 X. Lang, A. Hirata, T. Fujita, M. Chen, *NAT NANOTECHNOL*, 2011, 6, 232.
- 7 G.A. Snook, P. Kao, A.S. Best, *J POWER SOURCES*, 2011, 196, 1.
- 8 Q. Wang, L. Zhu, L. Sun, Y. Liu, L. Jiao, *J MATER CHEM A*, 2015, 3, 982.
- 9 G. Zhang, X.W.D. Lou, *ADV MATER*, 2013, 25, 976.
- 10 A. Pendashteh, M. S. Rahmanifar, R. B. Kanerc, M. F. Mousavi, *CHEM COMMUN*, 2014, 50, 1972.
- 11 Q. Wang, L. Zhu, L. Sun, Y. Liu, L. Jiao, *J MATER CHEM A*, 2015, 3, 982.
- 12 F. Yang, J. Yao, F. Liu, H. He, M. Zhou, P. Xiao and Y. Zhang, *J. Mater. Chem. A*, 2013, 1, 594.

- 13 Y. Sharma, N. Sharma, G. V. S. Rao, and B. V. R. Chowdari, *Journal of Power Sources*, 2007, 1, 495.
- 14 R. Tenne, *Nat. Nanotechnol.*, 2006, 1, 103.
- 15 C. Guan, J.P. Liu, C.W. Cheng, H.X. Li, X.L. Li, W.W. Zhou, H. Zhang, H. J. Fan, *Energy Environ. Sci.*, 2011, 4, 4496.
- 16 H. Zhang, Y. Chen, W. Wang, G. Zhang, M. Zhuo, H. Zhang, T. Yang, Q. Li, and T. Wang, *J. Mater. Chem. A*, 2013, 1, 8593.
- 17 G. Zhang, T. Wang, X. Yu, H. Zhang, H. Duan, B. Lu, *Nano Energy*, 2013, 2, 586.
- 18 V. Huang, S. Wu, M. E. Orazem, N. P'eb'ere, B. Tribollet, V. Vivier, *Electrochimica Acta*, 2011, 56, 8048.
- 19 X. D. Zhao, H. M. Fan, J. Luo, J. Ding, X. Y. Liu, B. S. Zou, Y. P. Feng, *Adv. Funct. Mater.* 2011, 21, 184.
- 20 G. Q. Zhang, H. B. Wu, H. E. Hoster, M. B. Chan-Park, X. W. Lou, *Energy Environ. Sci.* 2012, 5, 9453.
- 21 B. Guan, D. Guo, L. Hu, G. Zhang, T. Fu, W. Ren, J. Li, and Q. Li, *J. Mater. Chem. A*. 2014, 38, 16116
- 22 L. Mei, T. Yang, C. Xu, M. Zhang, L. Chen, Q. Li, and T. Wang, *Nano Energy*, 2014, 3, 36
- 23 G. Q. Zhang, H. B. Wu, H. E. Hoster, M. B. Chan-Park, and X. W. D. Lou, *Energy Environ. Sci.*, 2012, 5, 9453
- 24 G. H. Zhang, T. Wang, X. Z. Yu, H. N. Zhang, H.G. Duan, B. Lu, *Nano Energy*, 2013, 2, 586
- 25 L. Q. Mai, A. M. Khan, X. Tian, K. M. Hercule, Y. L. Zhao, X. Lin and X. Xu, *Nat. Commun*, 2013, 4, 2923
- 26 L. Q. Mai, F. Yang, Y. L. Zhao, X. Xu, L. Xu and Y. Z. Luo, *Nat. Commun*, 2011, 2, 381
- 27 S. Chen, J. Zhu, X. Wu, Q. Han, and X. Wang, *ACS Nano*, 2010, 4, 2822-2830